Available online at www.sciencedirect.com
SCIENCE DIRECT
Coordination Chemistry Reviews 250 (2006) 1783–1791
COORDINATION CHEMISTRY REVIEWS
www.elsevier.com/locate/ccr

Review

# Ultrafast dynamics of ligand-field excited states

Eric A. Juban, Amanda L. Smeigh, Jeremy E. Monat [1], James K. McCusker *

*Department of Chemistry, Michigan State University, East Lansing, MI 48824, United States*

Received 2 November 2005; accepted 10 February 2006
Available online 6 March 2006

## Contents



## Abstract

Ultrafast time-resolved spectroscopic methods have been used to probe the dynamics associated with ligand-field excited states in complexes of $Cr^{III}$ and $Fe^{II}$. In the former case, $Cr(acac)_3$ (where acac is the monodeprotonated form of acetylacetonate) serves as a prototype for studying the $^4T_2 \rightarrow {}^2E$ conversion endemic to complexes of this ion. The data reveal that formation of the $^2E$ state occurs faster than the instrumental time resolution of ca. 100 fs, implying a rate constant for intersystem crossing of $k_{ISC} > 10^{13}\ s^{-1}$. Subtle changes observed in the differential absorption spectra were attributed to vibrational cooling in the $^2E$ state having a time constant of $1.1 \pm 0.1$ ps. The role of low-lying ligand-field states as highly efficient deactivation pathways for higher-lying charge-transfer states was demonstrated in low-spin $Fe^{II}$ polypyridyl complexes. Following $^1A_1 \rightarrow {}^1$MLCT excitation, the ligand-field manifold is accessed with a time constant of ~100 fs. This pattern was observed for several different complexes, suggesting it is a general feature of this class of molecules. Dynamics subsequent to populating the ligand-field manifold are ill-defined at present but are presumed to consist of a barrierless evolution through a series of highly mixed ligand-field states, ultimately leading to the formation of the $^5T_2$ state as the lowest-energy excited state on the sub-picosecond time scale. This observation has important implications for the use of such complexes as sensitizers in photovoltaic applications.


*Keywords:* Ultrafast dynamics; Photophysics; Transition metal; Intersystem crossing; Vibrational relaxation

## 1. Introduction

The presence of ligand-field states – electronic states that derive largely from the d orbitals – is a unique defining feature of the photophysics and photochemistry of transition metal complexes [1]. Excited ligand-field states are responsible for a wide range of reactivity, most notably photosubstitution and

* Corresponding author. Tel.: +1 517 3559715; fax: +1 517 3559715.
*E-mail address:* jkm@cem.msu.edu (J.K. McCusker).
[1] Present address: Research and Technology Department, Indian Head Division, Naval Surface Warfare Center, Indian Head, MD 20640-1542, United States.

0010-8545/$ – see front matter © 2006 Elsevier B.V. All rights reserved.
doi:10.1016/j.ccr.2006.02.010

photoisomerization. Although charge-transfer states are most commonly associated with excited-state electron transfer, ligand-field states can also engage in photoredox chemistry [2]. The physiochemical properties of ligand-field states have been extensively investigated using an enormous range of spectroscopic probes. One frontier that remains is the application of the (relatively) recent technique of ultrafast spectroscopy. The ability to study the photophysical properties of molecules on time scales comparable to nuclear motion has revolutionized current thinking about the factors which govern the photo-induced dynamics of systems ranging from gas-phase diatomics to proteins [3]. The study of transition metal photophysics on the sub-picosecond time scale is a rapidly developing area of physical–inorganic chemistry [4,5] and holds considerable promise for advancing our fundamental understanding of excited-state electronic structure and reactivity. To date, the overwhelming majority of work in this field has involved the study of charge-transfer chromophores. With this contribution, we shift the focus to the ligand-field excited states of coordination compounds.

There are numerous technical challenges associated with the application of ultrafast spectroscopic methods to the study of photophysics of ligand-field excited states. First and foremost is the small absorption cross-section characteristic of such states: whereas charge-transfer transitions typically possess extinction coefficients on the order of $10^4\ M^{-1}\ cm^{-1}$, d–d bands are usually less intense by a factor of one hundred or more. This, coupled with the small path length cells required for sub-picosecond time resolution [6] translates into high sample concentrations and generally weak transient absorption features. Furthermore, the ability to selectively excite into a d–d band can be hindered by the presence of other absorptions with larger oscillator strengths (e.g., charge-transfer transitions). Given that ultrafast time resolution makes a wide range of molecular processes experimentally observable, excitation into states other than the one(s) of interest can significantly complicate the interpretation of data. Finally, the tendency for ligand-field excited states to undergo photochemistry can give rise to sample degradation during data acquisition. Judicious choices about which molecules to study must therefore be made in the initial stages of this research effort.

Herein we summarize work carried out on systems put forward as prototypes for the $d^3$ and $d^6$ configurations. First, results from a femtosecond time-resolved absorption study of $Cr(acac)_3$ will be described [7]. This compound possesses a number of features that help to circumvent the problems alluded to in the preceding paragraph. In particular, its well-isolated $^4A_2 \rightarrow {}^4T_2$ absorption combined with its relatively low quantum yield for photosubtitution [8] allows facile access to the lowest portion of the ligand-field manifold without the added complication of photochemical reactivity. The photophysics endemic to the $d^6$ configuration have been examined using $Fe^{II}$ polypyridyl complexes as the template [9]. In this case the initial excitation is charge-transfer, but the optical properties of the molecules are such that unambiguous characterization of the lower-lying excited ligand-field terms is achieved. The results on both systems demonstrate that interconversion among excited ligand-field states is kinetically competitive with other processes such as vibrational relaxation. Taken together, these observations point toward a need to re-evaluate current models that exist to describe excited-state evolution in transition metal-containing systems.

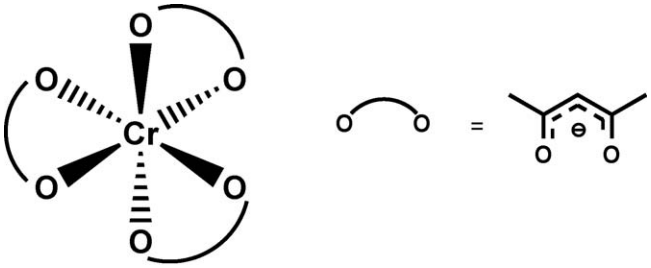


Drawing 1. Molecular structure of $Cr(acac)_3$.

## 2. Ultrafast dynamics of $Cr(acac)_3$

### 2.1. Basic spectroscopy

The electronic absorption spectrum of $Cr(acac)_3$ (Drawing 1) in $CH_3CN$ solution is shown in Fig. 1. It consists of a weak band centered near 560 nm ($\varepsilon \approx 50\ M^{-1}\ cm^{-1}$) that is easily assigned as the $^4A_2 \rightarrow {}^4T_2$ absorption (in the limit of O symmetry). The $^4A_2 \rightarrow {}^4T_1$ transition can be seen as a weak shoulder at higher energy, but is largely obscured by an intense feature at 336 nm assignable to a charge-transfer transition (most likely $^4A_2 \rightarrow {}^4$LMCT). The lowest energy excited state of $Cr(acac)_3$ is the $^2E$ state as evidenced by the narrow emission feature detected in a low-temperature glass (Fig. 1). Time-resolved emission measurements revealed a lifetime on the order of hundreds of microseconds, consistent with a $^2E$ assignment for the emissive state.

Data from time-resolved absorption measurements following ~100 fs excitation on the low-energy shoulder of the $^4A_2 \rightarrow {}^4T_2$ transition are summarized in Fig. 2. Both single-wavelength and full-spectrum data were acquired in order to fully characterize

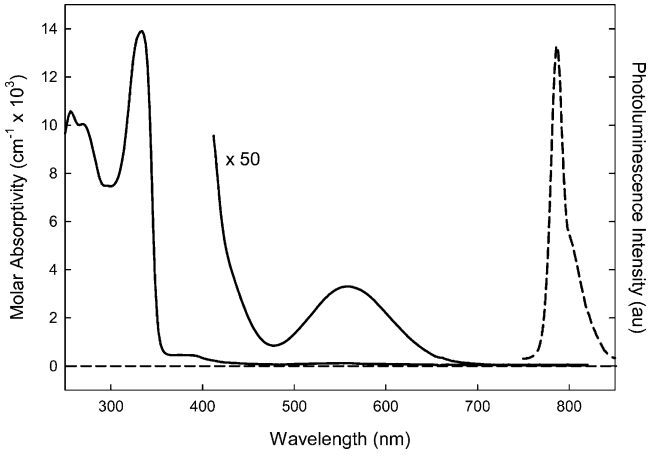


Fig. 1. Electronic absorption spectrum of $Cr(acac)_3$ in $CH_3CN$ solution (solid line). The emission spectrum (dashed line), acquired in a 4:1 EtOH/MeOH glass at 90 K, arises from the $^2E \rightarrow {}^4A_2$ transition in the compound.

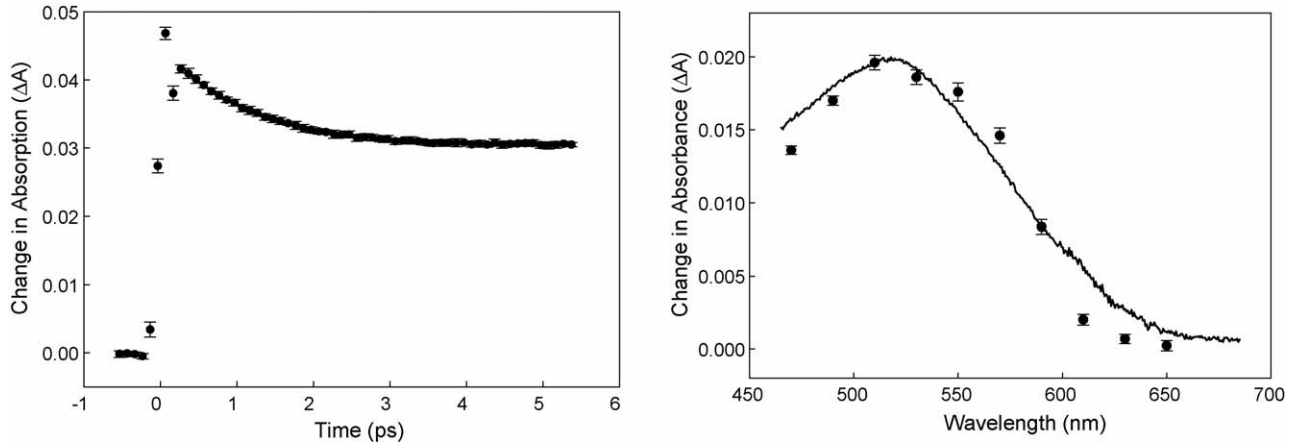


Fig. 2. Femtosecond time-resolved absorption data for $Cr(acac)_3$ in $CH_3CN$ solution following ~100 fs excitation at 625 nm. Left: single-wavelength kinetics trace at 480 nm. The solid line corresponds to a fit to a single exponential decay to a baseline offset with $\tau = 1.1 \pm 0.1$ ps. Right: full-spectrum acquired at $\Delta t = 5$ ps (solid line) superimposed on data collected at 90 K in a 4:1 EtOH/MeOH glass on the nanosecond time scale (data points). The latter corresponds to the excited-state difference spectrum of the $^2E$ state.

the kinetics and overall spectroscopic signatures, respectively, of the excited states being probed. The kinetics trace reveals single-exponential decay behavior with a time constant of $1.1 \pm 0.1$ ps. This feature does not return to baseline, but rather decays to a significant absorptive offset that persists for hundreds of picoseconds. A differential absorption spectrum acquired at a time delay $\Delta t = 5$ ps (i.e., after the decay is complete but prior to any evolution of the long-lived signal) is shown on the right side of Fig. 2. Superimposed on this trace are data acquired on $Cr(acac)_3$ on the nanosecond time scale in a low-temperature glass. The latter spectrum corresponds to a transition from the $^2E$ excited state to a higher energy charge-transfer state (presumably LMCT in nature). The similarity between it and the time-resolved data at $\Delta t = 5$ ps allows us to establish the presence of the $^2E$ state in the ultrafast experiment by the end of the kinetic feature shown on the left. It should be emphasized that this does not imply that the $1.1 \pm 0.1$ ps process monitored at 480 nm corresponds to the formation of the $^2E$ state. At this point we can only state that, whatever the decay process reflects, the $^2E$ state is established upon its completion.

The relative simplicity of the electronic structure of $Cr(acac)_3$, coupled with the spectral isolation of the $^4A_2 \rightarrow {}^4T_2$ absorption feature, limits the number of possibilities for an assignment of the kinetics displayed in Fig. 2. These are (1) vibrational cooling within the $^4T_2$ state, (2) $^4T_2 \rightarrow {}^2E$ conversion, (3) vibrational cooling within the $^2E$ state, or (4) a combination of any or all of the above. Each scheme has different implications concerning the relative rates of intramolecular processes occurring in $Cr(acac)_3$ as well as what is and is not spectroscopically observable. For example, option (3) would imply a $^4T_2 \rightarrow {}^2E$ conversion whose rate exceeds our time resolution, whereas option (1) would require that the $^4T_2$ and $^2E$ states have an isosbestic at 480 nm. Regardless, the data shown in Fig. 2 are insufficient to distinguish among these various scenarios and illustrate the general need for an extensive set of experiments in order to understand the photophysics of metal complexes on ultrafast time scales.

### 2.2. Spectral evolution at early times

Since the data at $\Delta t = 5$ ps clearly show that the $^2E$ state is present upon completion of the 1.1 ps decay in Fig. 2, attributing the kinetics to dynamics associated with the $^4T_2$ state (option (1) and/or (2) in the above) hinge upon establishing the presence of another electronic state. Unlike charge-transfer spectra that can be simulated using spectroelectrochemistry [4] the spectra of excited ligand-field states cannot be easily predicted (one notable exception being the $Fe^{II}$ system discussed later). We must therefore rely largely on chemical intuition to anticipate what absorption properties various excited states might possess. On this basis, it is our expectation that the excited-state absorption spectra of the $^4T_2$ state, which derives from a $(t_2)^2(e)^1$ configuration, and the $^2E$ state, arising from a $(t_2)^3$ configuration, will be different from each other. While we cannot infer anything about the specific nature of such differences, we nevertheless expect that the spectral signature of the $^4T_2$ state should be distinct in some way from that of the $^2E$ state. Data acquired over a broad range of probe wavelengths over the course of the 1.1 ps decay should allow us to discern the presence or absence of the $^4T_2$ state in the observed dynamics.

Full-spectrum data acquired at various time delays over the first several ps following $^4A_2 \rightarrow {}^4T_2$ excitation are shown in Fig. 3. It can be seen that, with the exception of a slight narrowing of the spectrum and a subtle red shift, the spectra at the earliest times available to us are essentially indistinguishable with that of the $^2E$ state at $\Delta t \geq 5$ ps. Based on the significant difference in electronic configurations between the two terms in question, we believe that this observation rules out any scenario involving the $^4T_2$ state, at least on this time scale. This implies that the dynamics illustrated in Fig. 2 are occurring subsequent to formation of the $^2E$ state. Given our ~100 fs time resolution, intersystem crossing associated with the $^4T_2 \rightarrow {}^2E$ conversion therefore occurs with a rate constant $k_{ISC} > 10^{13}\ s^{-1}$ [10].

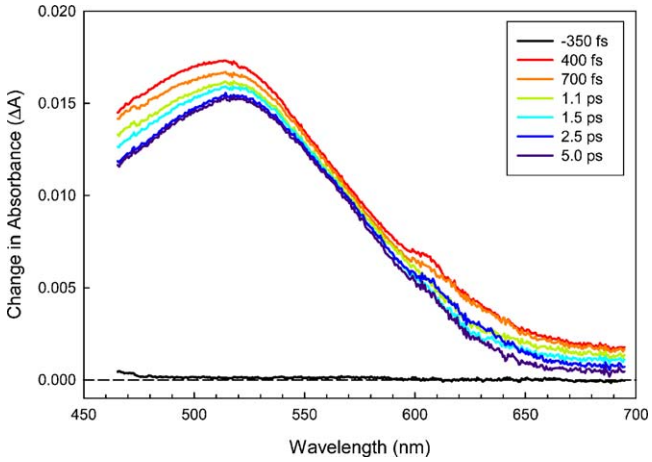


Fig. 3. Time-resolved absorption difference spectra for $Cr(acac)_3$ in $CH_3CN$ solution following ~100 fs excitation at 625 nm. The inset numbers indicate delay times for the probe beam relative to excitation at $\Delta t = 0$.

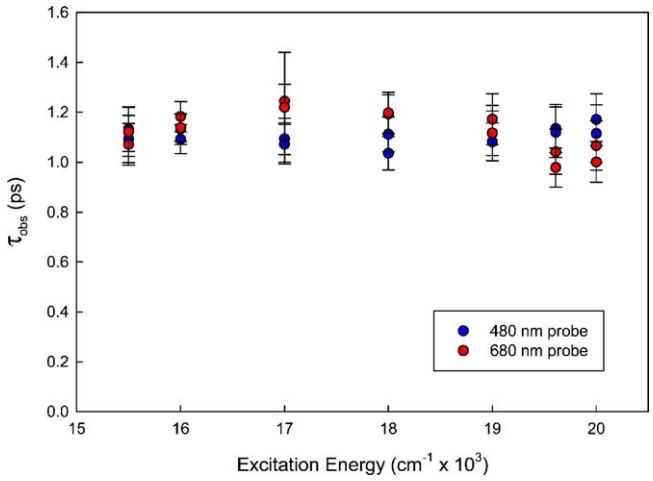


Fig. 4. Time constant for relaxation within the $^2E$ state of $Cr(acac)_3$ in $CH_3CN$ solution. Only two probe wavelengths are shown, but similar results were found for probe wavelengths across the entire excited-state absorption profile.

### 2.3. Variable-pump/variable-probe measurements

Having ruled out direct observation of the $^4T_2$ state, the only option remaining of those outlined above for assigning the $1.1 \pm 0.1$ ps process is vibrational relaxation in the $^2E$ state. Vibrational relaxation dynamics have been the subject of numerous studies over the years [11]. While the vast majority of work has focused on small molecules, there have been a number of reports published detailing vibrational processes in transition metal complexes [12]. Most of these have dealt with metal carbonyls, although more recent efforts have begun to broaden this horizon [13]. The spectral evolution shown in Fig. 3 has all of the qualitative features one associates with vibrational relaxation dynamics, in particular the sharpening of the spectrum that is giving rise to the observed kinetics.

One of the diagnostics used to infer vibrational relaxation dynamics from differential electronic absorption spectra is a dependence of the observed kinetics on the pump and/or probe wavelength. A more detailed discussion of both the origin and consequence of these effects can be found elsewhere [7]. Fig. 4 shows the fitted time constant for $Cr(acac)_3$ as a function of pump wavelength across the entire $^4A_2 \rightarrow {}^4T_2$ profile for two probe wavelengths at either edge of the spectra shown in Fig. 3. Although there are some small fluctuations, we can discern no systematic variations in the measured value of $\tau$ that lie outside experimental error. We believe that the absence of any discernable trend in $\tau$ may be due to the lack of high-frequency oscillators in $Cr(acac)_3$, in contrast to metal carbonyls where such trends have been observed by other workers [12]. Additional studies are clearly needed in order to substantiate this hypothesis.

### 2.4. Dynamics associated with the $^4T_2$ state

Although we were unable to directly observe the initially formed $^4T_2$ state, the variable-pump wavelength studies do provide insight into the rate of vibrational relaxation on the $^4T_2$ surface. In Fig. 5 are plotted the initial amplitudes from the fits of the decay kinetics as a function of excitation wavelength across the $^4A_2 \rightarrow {}^4T_2$ absorption envelope (also included is a data point following charge-transfer excitation in the near ultra-violet, the details about which are beyond the scope of this report). The amplitudes have been normalized to their long-lived values (i.e., $\Delta t > 5$ ps, designated by $a_0$), a procedure that corrects the data for any changes in pump/probe cross-section, laser power, etc. from one pump/probe combination to the next. The data clearly show a systematic increase in the amplitude of the initial absorption cross-section as the excitation energy is increased. This increase in amplitude occurs to the blue and to the red of the transient absorption maximum but dissipates near $\lambda_{max}$, indicating that the overall absorption profile is becoming broader with increasing excitation energy [14].

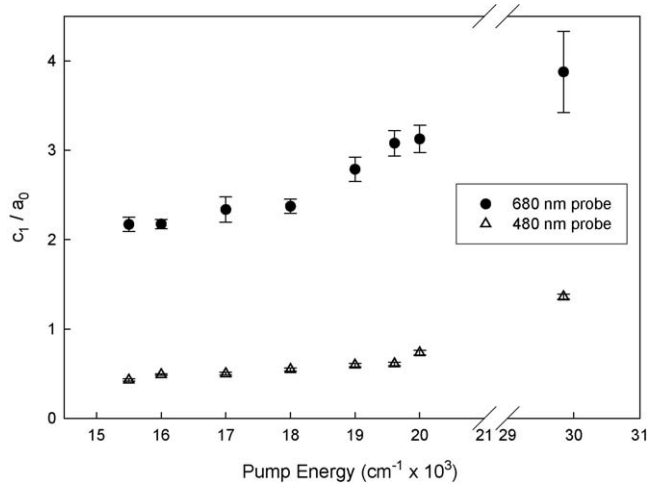


Fig. 5. Plot of the (normalized) transient absorption amplitude for relaxation within the $^2E$ state of $Cr(acac)_3$ at two different probe wavelengths as a function of excitation energy. The $y$-axis values were determined from single-exponential fits (e.g., Fig. 2, left) according to the equation $\Delta A = c_1 \exp\{-kt\} + a_0$, where $k$ is the fitted rate constant for decay and $a_0$ is the baseline offset (i.e., the absorbance of the $^2E$ state subsequent to vibrational cooling).

This observation can be interpreted in the following manner. We have already assigned the observed spectral narrowing to vibrational cooling in the $^2$E state. The breadth of the transient absorption feature at very early times ($\Delta t < 1$ ps) can be viewed as a measure of the amount of energy being dissipated. In other words, the spectral width relative to what is observed for the fully thermalized state (i.e., $\Delta t > 5$ ps) reflects how high on the $^2$E potential the system has been placed. If vibrational relaxation on the initially formed $^4T_2$ surface were faster than intersystem crossing, the crossover point would be invariant with excitation wavelength: the molecule would first fully thermalize on the $^4T_2$ surface, then intersystem cross to the $^2$E state at or near the $v = 0$ vibrational level of the $^4T_2$. Under this scenario, the breadth of the $^2$E absorption should be independent of excitation wavelength, since it will always be formed with the same amount of excess energy corresponding to where the zero-point of the $^4T_2$ intersects the $^2$E state. The fact that the spectrum does broaden significantly and systematically with increasing excitation energy indicates that the $^4T_2 \rightarrow {}^2$E conversion must occur prior to significant evolution on the $^4T_2$ surface in order for the excess excitation energy to be manifested in the absorption profile of the $^2$E state. This straightforward conclusion lends additional support to some of our previous assertions and allows us to infer that intersystem crossing is kinetically competitive with vibrational cooling in the $^4T_2$ state.

### 2.5. Summary: ligand-field dynamics of Cr(acac)$_3$

The data described in the preceding sections allow us to construct a Jablonski-type diagram summarizing the photophysics of Cr(acac)$_3$ (Fig. 6). The most striking feature about these results is the extremely fast rate of intersystem crossing. In particular, the fact that ISC is faster than vibrational cooling in the $^4T_2$ state signifies a break-down in the so-called cascade model typically invoked to model excited-state evolution, in which intersystem crossing is assumed to be the slowest of the three primary photophysical processes (vibrational relaxation, internal conversion, and intersystem crossing). Ultrafast measurements are currently underway on several other $Cr^{III}$ complexes in an effort to assess the generality of the dynamics found for Cr(acac)$_3$.

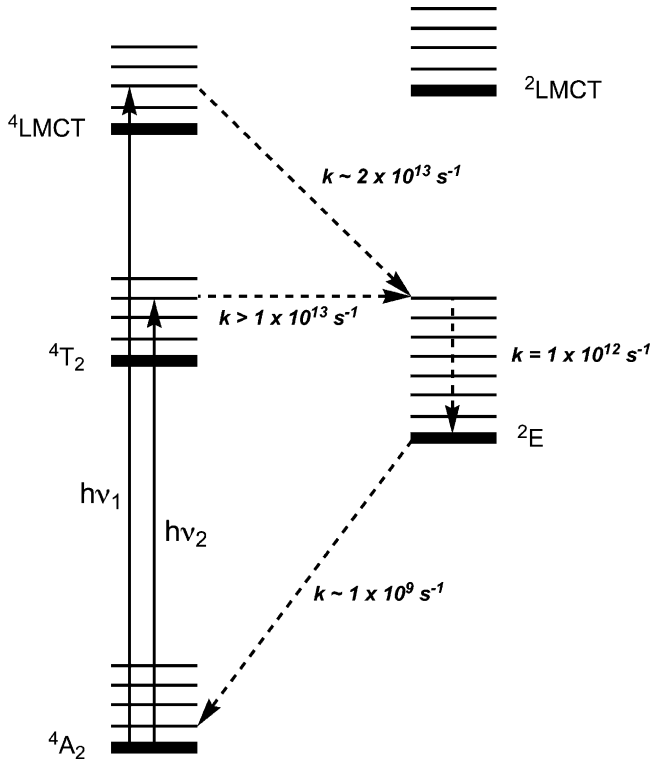


Fig. 6. Simplified Jablonski diagram illustrating the excited-state dynamics observed for Cr(acac)$_3$ in $CH_3CN$ solution. A discussion of the kinetics observed following charge-transfer excitation can be found in Ref. [7].

## 3. Photophysics of $Fe^{II}$ polypyridyl complexes

### 3.1. Identification of charge-transfer versus ligand-field optical features

Unlike the well-isolated features of Cr(acac)$_3$, study of the ultrafast ligand-field photophysics of this class of compounds is complicated by the presence of intense MLCT absorptions that obscure the $^1A_1 \rightarrow {}^1T_1$ and $^1A_1 \rightarrow {}^1T_2$ bands expected for the low-spin $d^6$ configuration. In addition, the non-emissive nature of these molecules adds another level of ambiguity for identifying the lowest-energy excited state of these systems. To circumvent this latter problem, we chose to study $[Fe(tren(py)_3)]^{2+}$ as our prototype (Drawing 2) [9]. This compound presents a ligand-field comprised of three pyridyl and three imine nitrogens: this places the compound just to the low-spin side of the spin-crossover point with the $^5T_2$ state as its lowest-energy excited state [15].

One issue of interest is simply the time scale on which the $^5T_2$ state is formed following excitation of the low-spin species. As was the case with Cr(acac)$_3$, this requires some knowledge of the absorption properties of the excited state that is ultimately formed, i.e., the $^5T_2$. As described by Drago and co-workers [16] and later by Hendrickson [17], substitution at the ortho position of the pyridyl ring introduces sufficient steric interactions to stabilize the high-spin $^5T_2$ state as the ground state of $[Fe(tren(6\text{-}Me\text{-}py)_3)]^{2+}$ (Drawing 2). Thus, the ground-state spectroscopic properties of $[Fe(tren(6\text{-}Me\text{-}py)_3)]^{2+}$ (Fig. 7, middle) will be essentially identical to those of the lowest energy excited state of

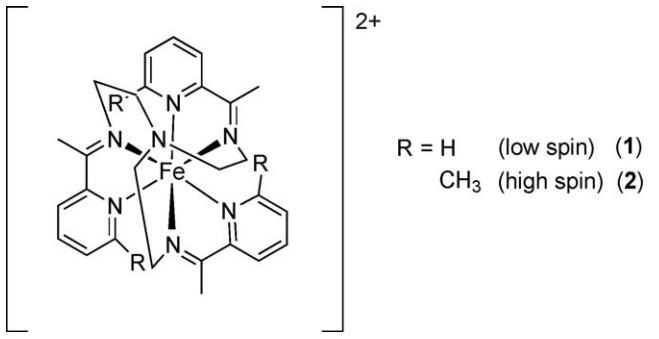


Drawing 2. Molecular structures of $[Fe(tren(py)_3)]^{2+}$ (R = H) and $[Fe(tren(6\text{-}Me\text{-}py)_3)]^{2+}$ (R = $CH_3$).

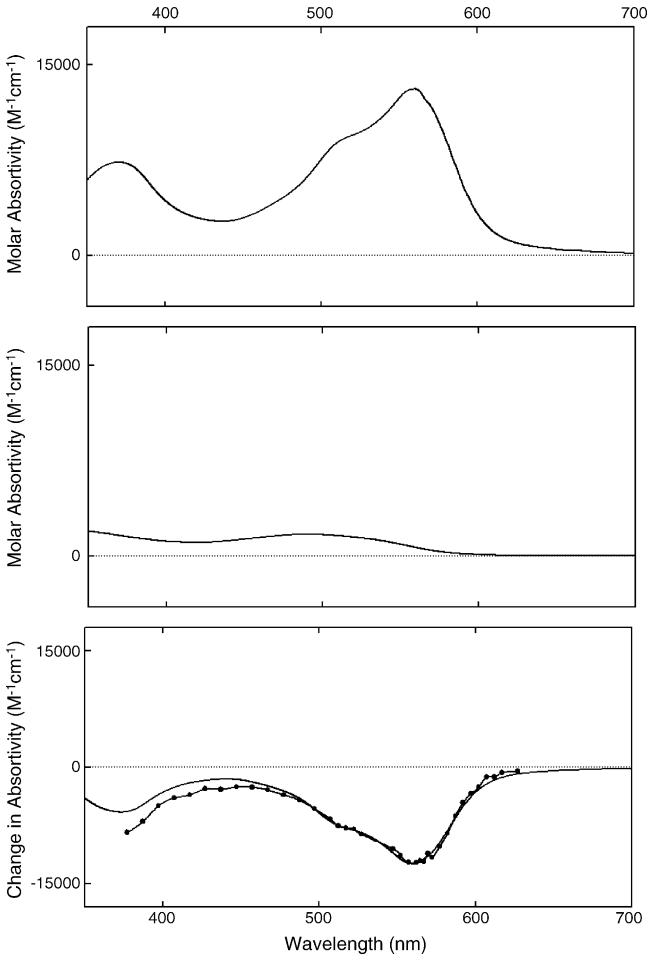


Fig. 7. Electronic absorption spectra of $[Fe(tren(py)_3)](PF_6)_2$ (top), $[Fe(tren(6\text{-}Me\text{-}py)_3)](PF_6)_2$ (middle), and their calculated difference spectrum (bottom, solid line). Also shown in the bottom panel (data points) is the nanosecond time-resolved difference spectrum obtained following excitation of $[Fe(tren(py)_3)]^{2+}$ in $CH_3CN$ solution.

$[Fe(tren(py)_3)]^{2+}$. This provides us with an unambiguous signature for the formation of the $^5T_2$ state following $^1A_1 \rightarrow {}^1$MLCT excitation of $[Fe(tren(py)_3)]^{2+}$ which we can utilize in much the same way as the low-temperature data were utilized for $Cr(acac)_3$ (Fig. 7, bottom).

Given the dominance of the MLCT feature in the absorption spectra of this entire class of compounds, a second question concerns the conversion between the charge-transfer and ligand-field manifolds. As mentioned previously, spectroelectrochemistry is a powerful tool for anticipating the optical properties of charge-transfer excited states. In the case of $[Fe(tren(py)_3)]^{2+}$, these data reveal that both the oxidative and reductive contributions to the charge-transfer manifold yield new absorptive features for $\lambda_{probe} > 600$ nm (Fig. 8). Inspection of the difference spectrum anticipated following formation of the $^5T_2$ state (Fig. 7, bottom) shows a net decrease in absorbance in this same wavelength region. Time-resolved kinetics monitoring this region of the spectrum should therefore provide some information concerning the kinetics of the MLCT-to-ligand-field conversion.

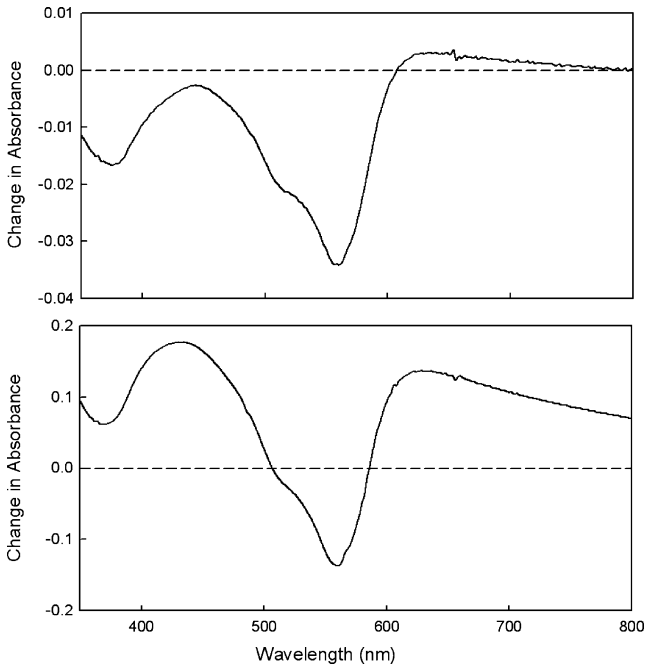


Fig. 8. Differential absorption spectra for $[Fe(tren(py)_3)]^{2+}$ in $CH_3CN$ solution following electrochemical oxidation (top) and reduction (bottom).

### 3.2. Ultrafast charge-transfer state deactivation

Single-wavelength kinetics data on $[Fe(tren(py)_3)]^{2+}$ in $CH_3CN$ solution at $\lambda_{probe} = 620$ nm following ~100 fs excitation at 400 nm are shown in Fig. 9. The data consist of an instrument-limited net absorptive feature which decays to a bleach (i.e., net absorptive loss) with a time constant of $\tau = 80 \pm 20$ fs (there is an additional evolution of the bleach feature at longer times having $\tau = 8 \pm 3$ ps that will be discussed in a later section). Qualitatively, the data are consistent with the expectations discussed above: an initial positive feature signaling the presence of a charge-transfer chromophore, followed by formation of a ligand-field state(s). Based on these data alone, no conclusions

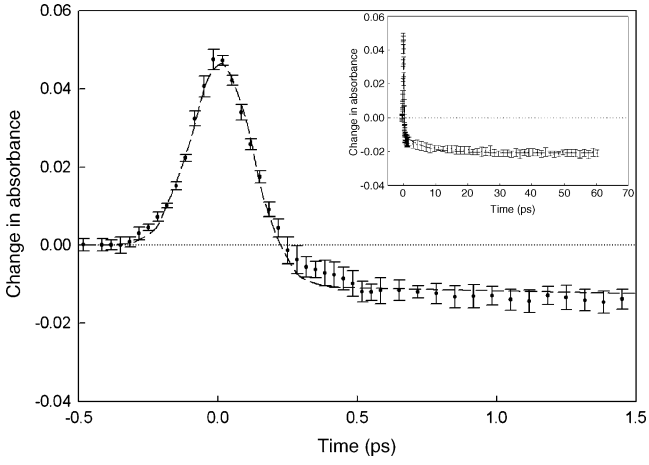


Fig. 9. Time-resolved differential absorption data for $[Fe(tren(py)_3)]^{2+}$ in $CH_3CN$ solution at 620 nm following ~100 fs excitation at 400 nm. The dashed line corresponds to a convolution of the instrument response function and a biexponential decay model with $\tau_1 = 80 \pm 20$ fs and $\tau_2 = 8 \pm 3$ ps (inset).

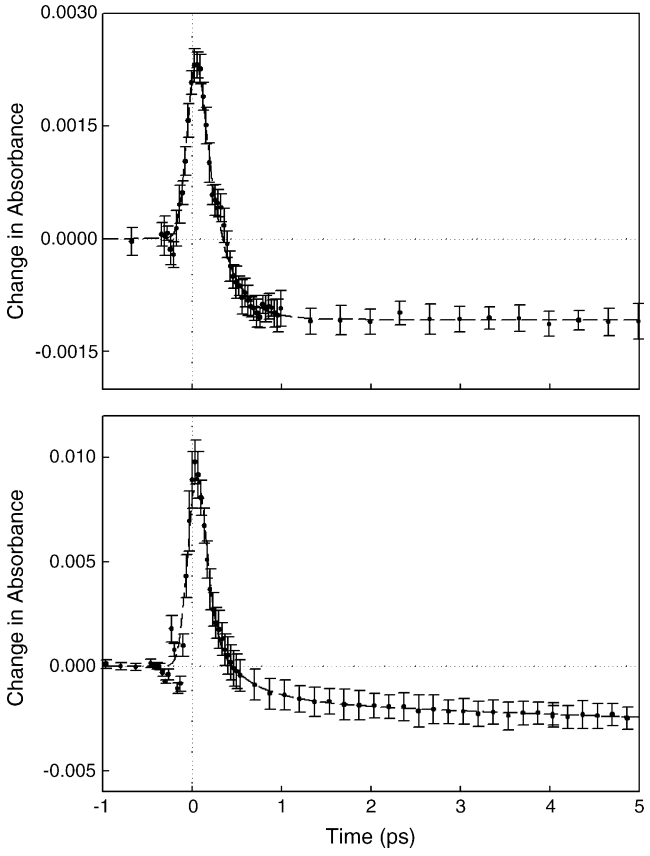


Fig. 10. Time-resolved differential absorption data for $[Fe(bpy)_3]^{2+}$ (top) and $Fe(bpy)_2(CN)_2$ (bottom) in $CH_3CN$ solution following ~100 fs excitaiton. Both complexes exhibit qualitatively similar dynamics with $\tau_1 < 100$ fs and $\tau_2 \sim 500$ fs. See Ref. [18] for further details.

can be drawn as to the nature of the ligand-field state(s) that are initially accessed; this point will be addressed in the next section. Nevertheless, the sub-100 fs time constant indicates an extremely short lifetime for the initially formed charge-transfer state.

Fig. 10 illustrates analogous data collected on $[Fe(bpy)_3]^{2+}$ and $Fe(bpy)_2(CN)_2$, representing two of several systems that we have examined [18]. A spectroscopic signature similar to that observed for $[Fe(tren(py)_3)]^{2+}$ is observed for all of these compounds. The rapid deactivation of the charge-transfer manifold ($\tau < 100$ fs) thus appears to be characteristic of this entire class of molecules. Although the focus of the present report is on the role of excited ligand-field states in ultrafast dynamics, the fact that the charge-transfer state(s) of $Fe^{II}$ polypyridyls are so short-lived has important implications for their use as sensitizers in photovoltaic applications [18–20].

### 3.3. Formation of the $^5T_2$ excited state

As was the case with $Cr(acac)_3$, the differential absorption spectrum of $[Fe(tren(py)_3)]^{2+}$ at long delay times (i.e., upon completion of all observed dynamics but prior to ground-state recovery) constitutes the "end-point" of excited-state evolution. In the case of the present compound, the availability of the high-spin analog allows us to unambiguously determine when the $^5T_2$

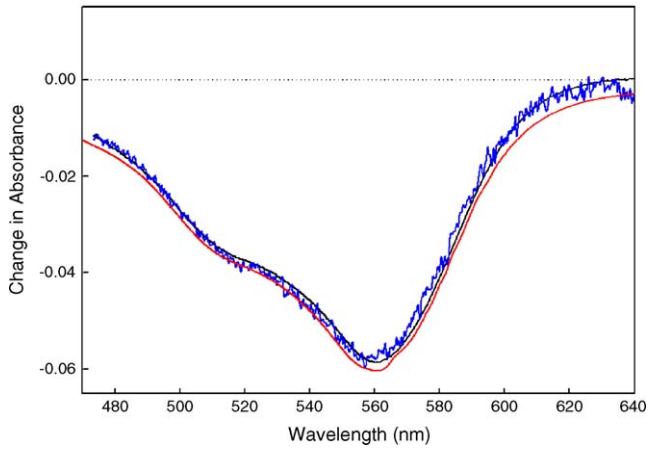


Fig. 11. Differential absorption spectra for $[Fe(tren(py)_3)]^{2+}$ in $CH_3CN$ solution following ~100 fs excitation at 400 nm. The spectra were acquired at delay times of $\Delta t = 700$ fs (black line) and 6 ps (blue line). The red line corresponds to the calculated low-spin/high-spin difference spectrum shown in the bottom panel of Fig. 7.

excited state of the low-spin complex is established. The plot in Fig. 11 shows a superposition of transient spectra acquired at time delays of $\Delta t = 700$ fs and 5 ps, along with the calculated high-spin/low-spin difference spectrum previously shown in Fig. 7. The agreement among all three spectra is quite good and provides compelling evidence that the $^5T_2$ state is well established by 700 fs following $^1A_1 \rightarrow {}^1$MLCT excitation of $[Fe(tren(py)_3)]^{2+}$ in room temperature solution.

Given the rate at which the $^5T_2$ state forms plus the fact that ground-state recovery in this compound occurs on the nanosecond time scale [21], the $8 \pm 3$ ps component evident in the inset of Fig. 9 cannot be associated a change in the electronic structure of $[Fe(tren(py)_3)]^{2+}$. By process of elimination, we therefore attribute this feature to vibrational relaxation in the $^5T_2$ state. The time scale is comparable to what was found for $Cr(acac)_3$; similar conclusions have been reached for $Ru^{II}$ polypyridyl complexes based on an analogous line of reasoning [4,22].

### 3.4. Mechanistic considerations

Our current picture for excited-state evolution following $^1A_1 \rightarrow {}^1$MLCT excitation of low-spin $Fe^{II}$ polypyridyl complexes is illustrated in Fig. 12. The diagram is unfortunately somewhat vague, but it does reflect the extent of detail currently supported by the available experimental data. For example, a $^3$MLCT state must certainly be present at an energy below the initially formed $^1$MLCT state, but we have no experimental data suggesting that such a state is even transiently populated. Similarly, it stands to reason that the $^1T_1$, $^1T_2$, $^3T_1$, and $^3T_2$ states – all of which energetically lie between the $^1$MLCT and $^5T_2$ states – are somehow involved in the relaxation process [23]. Apart from quantum mechanical considerations vis-à-vis spin–orbit coupling [24], our strongest experimental evidence for this is actually the rate at which the $^5T_2$ is formed. Given the zero-point energy of the $^5T_2$ state relative to the ground state in $[Fe(tren(py)_3)]^{2+}$, the excitation wavelength of 400 nm,

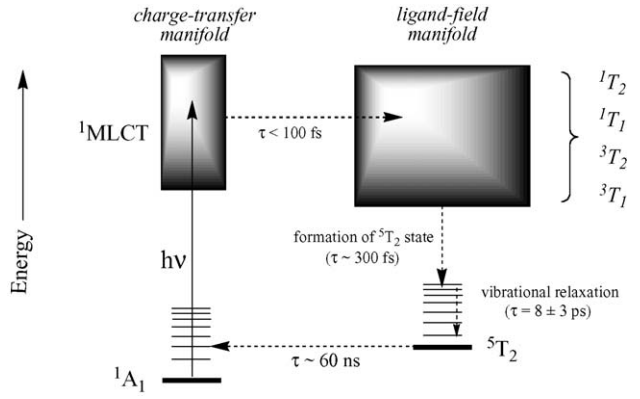


Fig. 12. Schematic diagram depicting the photophysics of $Fe^{II}$ polypyridyl complexes following $^1A_1 \rightarrow {}^1$MLCT excitation. The values for the various time constants are specific for $[Fe(tren(py)_3)]^{2+}$ in $CH_3CN$ solution, but the qualitative nature of these dynamics appears to be general for this class of molecules.

and a reasonable estimate of the total reorganization energy, the driving force for $^1$MLCT $\rightarrow {}^5T_2$ conversion is deep into the inverted region [25]: this is at odds with a rate constant in excess of $10^{12}$ $s^{-1}$. This observation is reminiscent of those made by Gray and co-workers concerning the photophysics of certain Ir complexes, which failed to show inverted behavior due to the involvement of higher-lying excited states in the relaxation mechanism [26]. Nevertheless, in the case of $Fe^{II}$ polypyridyls there is no direct evidence of their presence in the form of distinct, kinetic intermediates, hence the rather non-descript inclusion of these higher-lying ligand-field states in Fig. 12. Once the $^5T_2$ state is formed, subsequent relaxation back to the $^1A_1$ can be quantitatively described by non-radiative decay theory as has been shown in detail by Hauser, in particular [27].

The rapid formation of the $^5T_2$ state has several important consequences. First and foremost, the fact that a transition formally characterizable as a two-quantum spin change (i.e., $\Delta S = 2$) occurs on a sub-picosecond time scale underscores the notion that intersystem crossing in transition metal complexes can be exceedingly fast. Our data show that ISC can be orders of magnitude faster than vibrational relaxation dynamics, even in a relatively large molecule. A similar conclusion was gleaned in the case of $Cr(acac)_3$, where the $^4T_2 \rightarrow {}^2E$ conversion outpaced vibrational relaxation on the $^4T_2$ surface (Fig. 5). A related point is that spin selection rules do not appear to be a significant factor in the mechanism of excited-state evolution, at least in terms of dictating a sequence of states to be sampled along any given relaxation pathway. Rather, it would appear that the relative displacement of potential energy surfaces combined with the high density of states has a greater influence on the time-course of excited-state formation. We suspect it is likely the case that these latter two factors promote extensive mixing among the various excited states (both charge-transfer and ligand-field), leading to an essentially barrierless potential along which the system evolves toward the lowest-energy excited state. Computational efforts to explore this notion in greater detail are currently underway.

## 4. Concluding comments

It should be clearly stated that there is not enough information available on a wide enough range of molecules to make any broad generalizations concerning ultrafast dynamics in transition metal complexes. However, we have yet to come across a case in which an assumption that $k_{vib} > k_{IC} > k_{ISC}$ – which conforms to the conventional photophysical picture one gleans from textbooks – leads to the correct conclusions when it comes to a mechanistic description of excited-state formation. Our previous work on charge-transfer chromophores led us to this conclusion [4], and these initial efforts involving ligand-field excited states appear to be pointing in the same direction. The underlying reason(s) for these surprisingly fast rates of surface crossings remains an open question. For example, we have assumed approximate O symmetry for the sake of simplicity in the discussions presented above. However, the low-symmetry ligand fields of these molecules will lift the degeneracies of the states involved in the relaxation mechanisms shown above; the extent to which this is affecting the ultrafast dynamics of these systems is unclear. Nevertheless, given these findings it is our strong belief that mechanistic proposals for excited-state evolution must be made with extreme caution and a strict adherence to what the data indicate rather than on any presumption of the relative rates of various processes that might be involved.

## Acknowledgments

The authors wish to thank the National Science Foundation (Grant Nos. CHE-0316742 and CHE-0213505) and the Chemical Sciences, Geosciences, and Biosciences Division, Office of Basic Energy Sciences, Office of Science, U.S. Department of Energy (Grant No. DE-FG02-01ER15282) for financial support of this research.

## References

[1] G.J. Ferraudi, Elements of Inorganic Photochemistry, John Wiley and Sons, New York, 1988;
D.M. Roundhill, Photochemistry and Photophysics of Metal Complexes, Plenum Press, New York, 1994.
[2] B. Brunschwig, N. Sutin, J. Am. Chem. Soc. 100 (1978) 7568 (see also Chapter 2 in Roundhill (cf. [1])).
[3] For a few more recent, specific examples, see:
M. Dantus, A. Zewail, Chem. Rev. 104 (2004) 1717, and subsequent papers in that issue.
[4] J.K. McCusker, Acc. Chem. Res. 36 (2003) 876.
[5] A. Vlcek, Coord. Chem. Rev. 200 (2000) 933.
[6] The spectral bandwidth of a pulse at the transform limit is dictated by the Heisenberg relation $\Delta E \times \Delta t \sim h/2\pi$, implying that short pulses have very large bandwidths. Consequently, many materials (e.g., solvents, glass walls of cuvettes, etc.) cause sub-picosecond pulses to become temporally broadened ("chirped") as they propagate through the medium. In order to minimize this effect, optical paths of 1 mm or less are typically used in these experiments.
[7] E.A. Juban, J.K. McCusker, J. Am. Chem. Soc. 127 (2005) 6857.
[8] E. Zinato, P. Riccieri, P.S. Sheridan, Inorg. Chem. 18 (1979) 720.
[9] J.E. Monat, J.K. McCusker, J. Am. Chem. Soc. 122 (2000) 4092.

[10] The failure to observe the $^4T_2$ state allows us to draw this conclusion concerning the rate of intersystem crossing in the case of $Cr(acac)_3$. However, in general time-resolved absorption is not the best method for definitively measuring $k_{ISC}$ (cf. [4]).
[11] J.C. Owrutsky, D. Raftery, R.M. Hochstrasser, Annu. Rev. Phys. Chem. 45 (1994) 519;
M.H. Cho, Phys. Chem. Commun. 5 (2002) 40;
R.M. Stratt, M. Maroncelli, J. Phys. Chem. 100 (1996) 12981;
K.D. Rector, M.D. Fayer, Int. Rev. Phys. Chem. 17 (1998) 261;
For a few more recent, specific examples, see:
T. Schrader, A. Sieg, F. Koller, W. Schreier, Q. An, W. Zinth, P. Gilch, Chem. Phys. Lett. 392 (2004) 358;
M. Khalil, N. Demirdoven, A. Tokmakoff, J. Chem. Phys. 121 (2004) 362;
J.B. Asbury, T. Steinel, M.D. Fayer, J. Phys. Chem. B 108 (2004) 6544.
[12] A few examples are:
A. Gabrielsson, P. Matousek, M. Towrie, F. Hartl, S. Zalis, A. Vlcek, J. Phys. Chem. A 109 (2005) 6147;
P. Portius, J.X. Yang, X.Z. Sun, D.C. Grills, P. Matousek, A.W. Parker, M. Towrie, M.W. George, J. Am. Chem. Soc. 126 (2004) 10713;
D.J. Liards, M. Busby, P. Matousek, M. Towrie, A. Vlcek, J. Phys. Chem. A 108 (2004) 2363;
M. Lee, C.B. Harris, J. Am. Chem. Soc. 111 (1989) 8963;
T. Lian, S.E. Bromberg, M. Asplund, H. Yang, C.B. Harris, J. Phys. Chem. 100 (1996) 11994;
S.K. Doorn, R.B. Dyer, P.O. Stoutland, W.H. Woodruff, J. Am. Chem. Soc. 115 (1993) 6398;
N.J. Tro, J.C. King, C.B. Harris, Inorg. Chim. Acta 229 (1995) 469.
[13] M.K. Kuimova, J. Dyer, M.W. George, D.C. Grills, J.M. Kelly, P. Matousek, A.W. Parker, X.Z. Sun, M. Towrie, A.M. Whelan, Chem. Commun. (2005) 1182;
M. Busby, P. Matousek, M. Towrie, A. Vlcek, J. Phys. Chem. A 109 (2005) 3000.
[14] A full spectrum acquired near $\Delta t = 0$ would afford similar information, but for various experimental reasons the effect is easier to discern from single-wavelength probe data (cf. [7]).
[15] Variable-temperature magnetic data on this and related compounds indicate that the zero-point energy difference between the $^1A_1$ ground state and $^5T_2$ excited state in $[Fe(tren(py)_3)]^{2+}$ is $\approx 1000\,cm^{-1}$ (cf. [16,17]).
[16] M.A. Hoselton, L.J. Wilson, R.S. Drago, J. Am. Chem. Soc. 97 (1975) 1722.
[17] A.J. Conti, C.-L. Xie, D.N. Hendrickson, J. Am. Chem. Soc. 111 (1989) 1171.
[18] A.L. Smeigh, J.K. McCusker, in preparation.
[19] D.F. Watson, G.J. Meyer, Annu. Rev. Phys. Chem. 56 (2005) 119, and references therein.
[20] S. Ferrere, B.A. Gregg, J. Am. Chem. Soc. 120 (1998) 843.
[21] The lifetime of the $^5T_2$ state of $[Fe(tren(py)_3)]^{2+}$ in fluid solution at room temperature is $60 \pm 5$ ns.
[22] The newly developed technique of femtosecond stimulated Raman scattering (FSRS) has recently been applied to the excited-state dynamics of $[Ru(bpy)_3]^{2+}$ in fluid solution. This method holds considerable promise for a much more detailed examination of vibrational relaxation dynamics on ultrashort time scales (R.A. Mathies, personal communication).
[23] A. Hauser, A. Vef, P. Adler, J. Chem. Phys. 95 (1991) 8710.
[24] Since there is no matrix element that provides for direct mixing between states differing by two spin quanta, one must invoke second-order spin–orbit interactions (i.e., $S = 0/S = 1$ and $S = 1/S = 2$) in order to realize a $\Delta S = 2$ conversion.
[25] This estimate is based on a combination of the excitation wavelength of 400 nm, the zero-point energy of the $^5T_2$ being $\sim 1000\,cm^{-1}$ above the ground state (Ref. [15]), and inner- and outer-sphere reorganization energies of 0.6 eV (J.K. McCusker, D.N. Hendrickson, unpublished results) and ~1 eV, respectively.
[26] L.S. Fox, M. Kozik, J.R. Winkler, H.B. Gray, Science 247 (1990) 1069.
[27] A. Hauser, Top. Curr. Chem. 234 (2004) 155;
A. Hauser, Comments Inorg. Chem. 17 (1995) 17;
A. Hauser, P. Adler, S. Deisenroth, P. Gutlich, C. Hennen, H. Spiering, A. Vef, Hyperfine Interact. 90 (1994) 77.